Basic Concepts for Simple and Complex Liquids

Jean-Louis Barrat and Jean-Pierre Hansen

CAMBRIDGE
UNIVERSITY PRESS

PUBLISHED BY THE PRESS SYNDICATE OF THE UNIVERSITY OF CAMBRIDGE
The Pitt Building, Trumpington Street, Cambridge, United Kingdom

CAMBRIDGE UNIVERSITY PRESS
The Edinburgh Building, Cambridge CB2 2RU, UK
40 West 20th Street, New York, NY 10011-4211, USA
477 Williamstown Road, Port Melbourne, VIC 3207, Australia
Ruiz de Alarcón 13, 28014 Madrid, Spain
Dock House, The Waterfront, Cape Town 8001, South Africa

http://www.cambridge.org

First published 2003

Printed in the United Kingdom at the University Press, Cambridge

Typefaces Times New Roman 10/13 pt and Univers *System* $\LaTeX\ 2_\varepsilon$ [TB]

A catalogue record for this book is available from the British Library

Library of Congress Cataloguing in Publication data

Barrat, Jean-Louis, 1964–
Basic concepts for simple and complex liquids / Jean-Louis Barrat and Jean-Pierre Hansen.
p. cm.
Includes bibliographical references and index.
ISBN 0-521-78344-5 – ISBN 0-521-78953-2 (pb.)
1. Liquids. 2. Complex fluids. I. Hansen, Jean Pierre. II. Title.
QC145.2 .B35 2003
530.4′2–dc21 2002031051

ISBN 0 521 78344 5 hardback
ISBN 0 521 78953 2 paperback

Contents

I Thermodynamics, structure and fluctuations

II Phase transitions

III Interfaces and inhomogeneous fluids

IV Dynamics

1 An introduction to liquid matter

One of the most remarkable observations in physical sciences or, for that matter, of everyday life, is that most substances, with a well defined chemical composition, can exist in one of several states, exhibiting very different physical properties on the macroscopic scale; moreover one can transform the substance from one state (or phase) to another, simply by varying thermodynamic conditions, like temperature or pressure. In other words, a collection of N molecules, where N is typically of the order of Avogadro's number $\mathcal{N}_{\mathrm{A}}$, will spontaneously assemble into macroscopic states of different symmetry and physical behaviour, depending on a limited number of thermodynamic parameters. The most common states are either solid or fluid in character, and are characterized by qualitatively different responses to an applied stress. At ambient temperatures, the solid states of matter are generally associated with the mineral world, while 'soft' matter, and in particular the liquid state, are more intimately related to life sciences. In fact it is generally accepted that life took its origin in the primordial oceans, thus underlining the importance of a full quantitative understanding of liquids. However, even for the simplest substances, there are at least two different fluid states, namely a low density 'volatile' gas (or vapour) phase, which condenses into a liquid phase of much higher density upon compression or cooling. For more complex substances, generally made up of highly anisotropic molecules or of flexible macromolecules, the liquid state itself exhibits a rich variety of structures and phases, often referred to as 'complex fluids'.

The present book deals with some of the more generic aspects and concepts of the liquid state of matter. Rather than attempting a systematic description of the many classes of liquids, this monograph intends to illustrate generic statistical concepts and theoretical tools on a number of examples, covering a wide range of structural, dynamic and phase behaviour. This introductory chapter offers general background material and basic facts of the liquid state. It is intended to provide the indispensable link between subsequent chapters devoted to more specific aspects and examples.

1.1 Fluid states of simple substances

Consider a sample of a simple, pure substance containing a large number ($N \simeq \mathcal{N}_A = 6.02 \times 10^{23}$) of identical molecules, say water or methane. At sufficiently high temperature T, and for not too high pressures P, the substance will be in its vapour or gas phase. Under ambient pressure, gases constitute a low density phase, where molecules are far apart, and undergo only occasional binary collisions, a regime well described by the ideal gas model and the Boltzmann kinetic equation. Molecular configurations are highly disordered, as signalled by a large entropy per molecule, S/N. All physical properties of this high temperature phase are invariant under arbitrary rotations and translations, i.e. the gas phase has full rotational and translational symmetry.

When the temperature is lowered, the vapour will generally condense into droplets of a much denser liquid phase, which has a greatly reduced entropy per molecule, indicating some degree of molecular order. In fact, if $v = V/N$ is the mean volume per molecule in the liquid, $\rho = 1/v$ is the number density and v_0 is the volume of one molecule, then the packing fraction

$$\phi = \frac{v_0}{v} = \rho v_0 \tag{1.1}$$

is typically of the order of 0.3–0.5 in most liquids. At such high densities neighbouring molecules almost touch, and form well defined shells of nearest neighbours around any given molecule, characteristic of short-range order. This order is, however, lost beyond a few intermolecular distances, so that liquids still preserve, in general, full rotational and translational symmetry, both locally and on macroscopic scales.

Upon further gradual cooling, the liquid samples will generally freeze into a crystalline solid phase, which is characterized by the appearance of long-range order, embodied in a periodic crystal lattice. The regularly spaced crystal planes will Bragg reflect X-rays, and the observed diffraction patterns obtained upon varying the crystal orientation in the X-ray beam allow an unambiguous characterization of the crystal structure. The appearance of long-range order leads to a reduction in symmetry: physical properties of the crystalline solid are now invariant only under a discrete set of reflections, rotations and translations constituting one of 230 possible space groups. The full rotational and translational symmetry of the fluid phases is said to be broken at the freezing transition to the low temperature crystal phase.

The scenario just described, which is generic for simple molecular systems, is summarized in the phase diagrams of figure 1.1, which represent three cuts through the surfaces in (P, T, ρ) space, bounding the gas, liquid and solid phases. It should be noted that the liquid state only occupies a relatively small portion in the three orthogonal planes, over a range of temperatures limited to $T_t \leq T \leq T_c$, where T_t denotes the triple point temperature, where all three phases coexist,

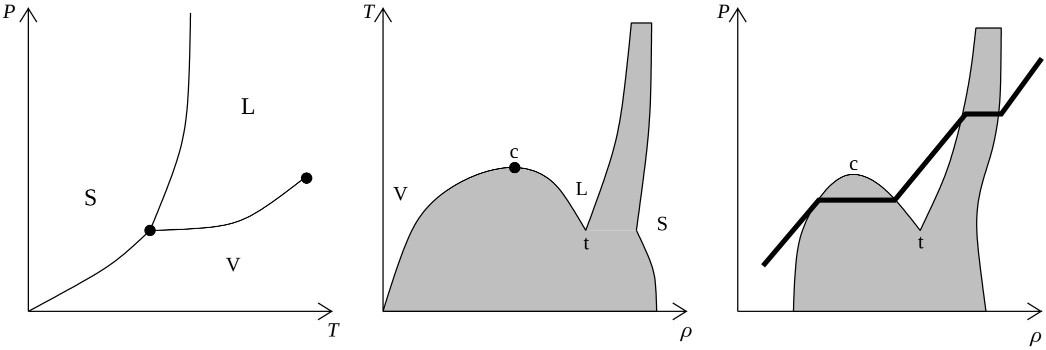

Figure 1.1. Schematic phase diagrams of a simple one-component substance, in the temperature (T)–pressure (P), density (ρ)–T and ρ–P planes. The shaded areas in the middle and right panels indicate regions of two-phase coexistence. The bold line in the right panel is an isotherm while t and c show the locations of the triple and critical points.

and T_c the critical point temperature, above which the liquid and the gas merge into a single fluid phase. The shaded areas in the (ρ, T) and (ρ, P) diagrams in figure 1.1 are two-phase regions: the corresponding thermodynamic states are either metastable or unstable, and will eventually lead to a separation into two coexisting stable phases. Examples of such states are superheated solids, supercooled liquids or supersaturated vapours. Depending on the degree of supersaturation, the latter will either form liquid droplets by a process of nucleation and growth (to be discussed in section 10.6), or undergo rapid spinodal decomposition (considered in section 9.3). Glasses constitute another particularly important class of metastable materials, often obtained by rapid cooling (or ‘quenching’) of a liquid well below its freezing temperature. Most substances form glasses only under rather extreme cooling conditions, but silicate melts, for instance, are easy and excellent glass-formers, as may be readily observed in the glass-blower’s workshop. Glasses are amorphous (‘structureless’) solids, which maintain the disordered structure and rotational/translational symmetry of liquids on the molecular scale, while exhibiting the rigidity (or resistance to shear deformation) of crystalline solids at the macroscopic level, although glasses may eventually flow over extremely long time scales[1].

The distinction between the spatial arrangements of molecules in gases, liquids and solids is illustrated very schematically in figure 1.2, which shows ‘snapshots’ of typical configurations of disc-like molecules in two-dimensional counterparts of the three phases. A quantitative measure of the local order on the molecular

---

[1] This slow flowing is often illustrated by medieval stained-glass windows, which should tend to be thicker at the bottom. Whether this is actually the case remains however a controversial question, see the discussion by E.D. Zanotto, *Am. J. Phys.* **66**, 392 (1998).

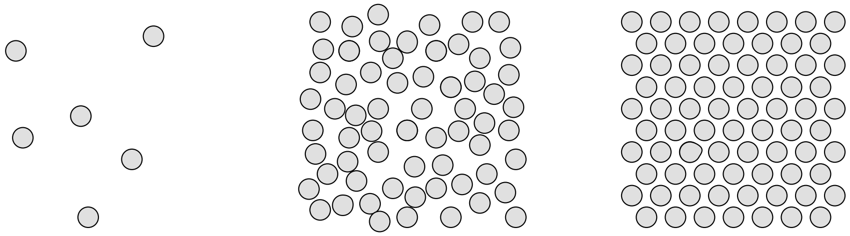

Figure 1.2. Typical atomic configurations in a gas (left), liquid (middle) and crystalline solid (right).

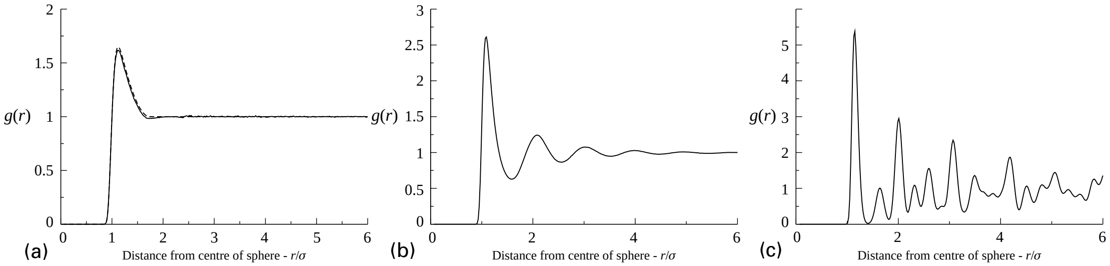

Figure 1.3. Typical pair distribution functions for (a) a gas, (b) a liquid and (c) a solid. These functions have been generated using a molecular dynamics simulation (see section 1.6) of atoms interacting through a Lennard-Jones potential (equation (1.9), figure 1.4). The Boltzmann factor for the Lennard-Jones potential has been superimposed on the gas phase distribution function (dashed curve). The thermodynamic states are: $T = 2\epsilon/k_{\mathrm{B}}$, $\rho\sigma^3 = 0.05$ (gas), $T = \epsilon/k_{\mathrm{B}}$, $\rho\sigma^3 = 0.8$ (liquid), $T = 0.2\epsilon/k_{\mathrm{B}}$, $\rho\sigma^3 = 0.9$ (solid).

scale is provided by the radial (or pair) distribution function $g(r)$, which characterizes the modulation of the local density $\rho(r)$ around a given molecule, as a function of the distance r from that molecule.

In the limit of an ideal gas of non-interacting (point) molecules, the local density, as seen from any one fixed molecule, is everywhere equal to its average ρ. In reality, molecules interact via a pair potential v, which, for spherical molecules, will only depend on the centre-to-centre distance r; even in a dilute gas, the local density around a fixed molecule will rapidly vanish for r less than the molecular diameter, and will be modulated by the Boltzmann factor $\exp(-\beta v(r))$, where $\beta = 1/k_{\mathrm{B}}T$. In other words

$$\rho(r) \equiv \rho g(r) = \rho \exp\left(-\beta v(r)\right) \tag{1.2}$$

In the liquid, however, the positions of neighbouring molecules are strongly correlated, leading to a modulation of $\rho(r)$ extending over a few molecular diameters, so that the radial distribution would behave as shown schematically in figure 1.3(b); the maxima may be associated with shells of neighbours, but the oscillations are rapidly damped, showing the gradual smearing out of short-range order; for $r \gg \sigma$, $g(r)$ goes to one, i.e. the local density around a fixed molecule tends rapidly to its macroscopic value ρ characteristic of a uniform (translationally invariant) fluid.

At the transition to the crystal phase the short-range order of the liquid grows spontaneously into full long-range order, signalled by well defined intermolecular distances and coordination numbers extending to macroscopic scales, which are characteristic of the periodic pattern of the crystal lattice. At zero temperature, this would reduce $g(r)$ to a sequence of δ-functions located at distances r dictated by the lattice geometry; at finite temperatures the δ-peaks are broadened by the thermal vibrations of molecules around their equilibrium lattice sites $\mathbf{R}_i$, as shown in figure 1.3(c). Note that since the crystal is anisotropic, its radial distribution function involves an average over all orientations of the lattice. An amorphous solid, however, is again isotropic, and its pair distribution function is generally difficult to distinguish from that of a liquid.

The two key macroscopic properties which distinguish liquids from their vapour, on the one hand, and fluids in general from solids, on the other hand, are cohesion and fluidity. Cohesion, shared by liquids and solids, is a consequence of intermolecular attractions, which lead to a significant lowering of the internal energy due to molecular clustering, compared to the gas phase; in the latter the thermal kinetic energy of the molecules is sufficient to overcome the short-range attraction, so that the molecules in the gas tend to occupy all the available volume. The fluidity of liquids and gases distinguishes them from the rigidity of crystalline solids. Consider the response to an applied stress (or force per unit area) characterized by the components of a macroscopic stress tensor. In the elastic regime of solids, corresponding to small strains or deformations, the components $\sigma_{\alpha\beta}$ of the stress tensor are proportional to those of the dimensionless symmetric strain tensor u, which measures the gradient of the displacement field $\mathbf{u}(\mathbf{r})$

$$u_{\alpha\beta} = \frac{1}{2}\left(\frac{\partial u_\alpha}{\partial x_\beta} + \frac{\partial u_\beta}{\partial x_\alpha}\right) \qquad \alpha, \beta = x, y, z \tag{1.3}$$

The coefficients of the linear relation between the components of the tensors σ and u are the components of a fourth rank tensor of elastic constants. The number of independent elastic constants is strongly reduced by symmetry considerations. In particular, for an isotropic solid, like a glass or a polycrystalline sample, the stress–strain relation reduces to

$$\sigma_{\alpha\beta} = B\delta_{\alpha\beta}u_{\zeta\zeta} + 2G\left(u_{\alpha\beta} - \frac{1}{3}\delta_{\alpha\beta}u_{\zeta\zeta}\right) \tag{1.4}$$

where B and G are the bulk and shear moduli, δ refers to the usual Kronecker symbol, and the Einstein convention of summation over repeated indices has been adopted. In particular, for a shear stress, the relation reads

$$\sigma_{xy} = 2Gu_{xy} \tag{1.5}$$

In fluids, however, the application of an external stress will result in flow characterized by a fluid velocity field **v**(**r**), rather than by an elastic displacement field **u**(**r**). The phenomenological linear relationship valid for the most common Newtonian fluids is now between the stress tensor and the rate of strain tensor

$$\gamma_{\alpha\beta} = \frac{1}{2}\left(\frac{\partial v_\alpha}{\partial x_\beta} + \frac{\partial v_\beta}{\partial x_\alpha}\right) \tag{1.6}$$

Since the velocity field is the time derivative of the displacement field, $\gamma_{\alpha\beta}$ has the dimension of inverse time or frequency. In the case of a shear stress, the elastic relation (1.5) is now replaced by

$$\sigma_{xy} = 2\eta\gamma_{xy} \tag{1.7}$$

where η is the shear viscosity, which characterizes the internal friction of the fluid. In contrast to the elastic response of a solid, the viscous flow in a liquid dissipates energy. In water, at room temperature, $\eta = 10^{-2}$ poise (1 poise $= 0.1$ kg/m s). On the molecular scale, the distinction between the rigidity of solids and the fluidity of liquids reflects itself in molecular diffusion. While in a solid, molecules remain localized in the vicinity of equilibrium lattice positions, except for occasional very rare jump events between neighbouring sites, the same molecules will gradually drift away from their initial positions in a liquid. The mean square displacement at time t of a molecule from its initial ($t = 0$) position is characterized, for times long compared to molecular time scales (which are typically of the order of femtoseconds), by Einstein's relation

$$\left\langle |\mathbf{r(t)} - \mathbf{r(0)}|^2 \right\rangle = 6Dt \qquad t \gg \tau \tag{1.8}$$

where the angular brackets denote a statistical average over initial conditions and D is the self-diffusion coefficient. For simple liquids, D is of the order of 10^{-9} m^2/s while in solids, D is several orders of magnitude smaller. Molecular diffusion will be studied in more detail in subsequent chapters. It is worth stressing already at this stage that, contrarily to viscous flow, molecular diffusion occurs spontaneously, in the absence of any externally applied stress, and is a consequence of thermal fluctuations and a signature of irreversible behaviour on mesoscopic and macroscopic scales. To conclude this introductory section it is important to underline that the perfect elastic behaviour of solids, embodied e.g. in equation (1.5), and the ideal Newtonian behaviour of liquids, described by equation (1.7), constitute ideal limits, and that many materials, either solid or liquid, exhibit macroscopic behaviour which may deviate very significantly from the above simple phenomenological laws. This is particularly true of complex fluids and soft condensed matter, as will become clearer in the course of this presentation.

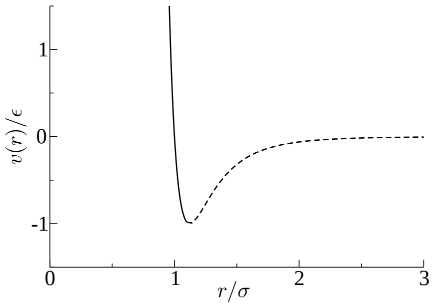

Figure 1.4. The Lennard-Jones potential, equation (1.9), as a function of interatomic distance.

1.2 From simple to complex fluids

The simple phase diagrams shown in figure 1.1, and the generic fluid behaviour sketched in section 1.1, are typical of 'simple' materials or substances composed of a single species of small, quasi-spherical molecules, say argon (Ar), nitrogen (N_2), methane (CH_4) or ammonia (NH_3). Argon atoms are strictly spherical and interact via a short-range repulsion, originating in the Pauli principle which opposes the overlap of electronic orbitals on neighbouring atoms, and longer ranged van der Waals–London dispersion forces, which are attractive; the dominant dispersion interaction decays like $1/r^6$. A convenient, semi-empirical representation incorporating these essential repulsive and attractive contributions is provided by the Lennard-Jones potential, shown in figure 1.4

$$v(r) = 4\epsilon\left(\left(\frac{\sigma}{r}\right)^{12} - \left(\frac{\sigma}{r}\right)^{6}\right) \tag{1.9}$$

where σ is the atomic diameter, and ϵ the depth of the attractive well; these two parameters are generally determined by fitting certain properties derived from the potential, like the second virial coefficient, to experimental data. For Ar, $\sigma \simeq 0.34$ nm and $\epsilon/k_B \simeq 120$ K[2]. Note that the simple $1/r^{12}$ form of the Lennard-Jones repulsion is for convenience; an exponential repulsion would be more realistic, but lacks the simplicity of an inverse power law.

The potential energy of interaction between two small polyatomic molecules is generally split into ν^2 spherically symmetric pair interactions between ν sites (e.g. the atomic nuclei) associated with each molecule. For highly polar molecules, the interaction sites carry electric charges, chosen such as to reproduce the known multipole moments of the molecule. An example illustrated in figure 1.5 is the simple point charge (SPC) model for water, involving $\nu = 3$ sites on each molecule.

An alternative, useful for quasi-spherical molecules, is to supplement a spherically symmetric potential, like the Lennard-Jones potential (1.9), with the

---

[2] Interaction energies are often expressed in temperature units, which gives a simple order of magnitude estimate for the triple point temperature.

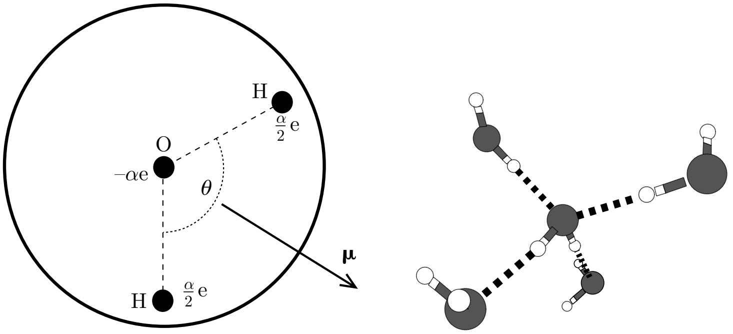

Figure 1.5. The simple point charge model of water (left): the oxygen atom carries an electric charge $-\alpha e$, and is the centre of a Lennard-Jones potential (cf. equation (1.9)); each hydrogen atom carries a charge $\alpha e/2$, with $\alpha = 0.8476$, and is situated at a distance $d = 0.1$ nm from the O atom; the HOH bond angle is 109.5°; this charge distribution gives rise to a dipole moment of magnitude $\mu = 2.3$ debye (H.J.C. Berendsen, J.R. Grigera and T.P. Straatsma, *J. Phys. Chem.* **91**, 6269 (1987)). The right-hand frame shows a typical hydrogen-bonded tetrahedral configuration of four molecules around a central water molecule. (Courtesy of D. Wales.)

anisotropic potential energy of electrostatic point multipoles. Molecules lacking a centre of symmetry, like NH_3 or CO, carry an electric dipole $\boldsymbol{\mu}$. The potential energy of two point dipoles $\boldsymbol{\mu}_1$ and $\boldsymbol{\mu}_2$ placed at a relative position $\mathbf{r} = \mathbf{r}_{12}$ is

$$v(\boldsymbol{\mu}_1, \boldsymbol{\mu}_2, \mathbf{r}) = -\sum_{\alpha,\beta} \mu_{1\alpha} T_{\alpha\beta}(\mathbf{r}) \mu_{2\beta} \tag{1.10}$$

where T is the dipole–dipole interaction tensor, with components

$$T_{\alpha\beta} = \nabla_\alpha \nabla_\beta \left(\frac{1}{4\pi\epsilon_0 r} \right) = \frac{1}{4\pi\epsilon_0 r^3} \left(\frac{r_\alpha r_\beta}{r^2} - \delta_{\alpha\beta} \right) \tag{1.11}$$

The dipole moment of a small molecule is of the order of the product of the elementary (proton) charge by a typical intramolecular length scale, say 0.1 nm, i.e. 1.6×10^{-29} C m in standard units. A convenient unit is the debye (1 D = $(1/3)10^{-29}$ C m); typical values for isolated molecules are $\mu = 1.08$ D for HCl, $\mu = 1.47$ D for NH_3 and $\mu = 1.85$ D for H_2O. The resulting dipolar interaction energy between two molecules is strong, $v/k_B \sim 10^4$ K for separations comparable to the molecular diameter; this is significantly larger than the van der Waals dispersion interaction. The dipolar interaction can be attractive (e.g. for head-to-tail configurations) or repulsive, depending on the mutual orientations of the vectors $\boldsymbol{\mu}_1$, $\boldsymbol{\mu}_2$ and $\mathbf{r}$. Dipolar interactions play a dominant part in some colloidal dispersions called ferrofluids, where colloidal particles with diameters $\sigma \simeq 10$ nm carry *magnetic* dipole moments[3]; the strong dipolar interactions lead

---

[3] For magnetic dipole moments the $1/4\pi\epsilon_0$ in equation (1.11) has to be replaced by its magnetic counterpart μ_0.

then to alignment of dipoles and chain formation, giving rise to very peculiar rheological properties. On the molecular scale, a particular form of chain or network formation is observed for some strongly polar molecules involving H^+ groups, the most prominent examples being HF, H_2O and H_3N. Because of the small size of the H atom, the electronegative atoms F, O or N of neighbouring molecules can approach very close to H^+ groups of a given molecule, such that the approximate point dipole picture to describe the charge distribution on the molecules breaks down. The true Coulomb interaction between two such molecules is stronger and highly directional, leading to the formation of hydrogen bonds with 'bond' energies intermediate between the usual intermolecular energies, and chemical bond energies (which are of the order of a few electronvolts). In the most important case of water, the intermolecular H-bond energy of a water dimer is typically of the order of $\epsilon_H/k_B = -3000$ K, i.e. much larger than thermal energies. It is also significantly larger, in absolute value, than the energy predicted by the point dipole approximation. The H-bond is highly directional, with the lowest energy achieved when the chemical (intramolecular) OH bond is aligned with the H–O 'bond' between the H on one molecule and the O on the neighbouring one; the corresponding optimal OH–O distance of the dimer is about 0.28 nm. This strong directionality, and the fact that the intramolecular HOH bond angle of water is 105°, very close to the tetrahedral value of 109°, leads to a network-like organization of H_2O molecules in ice, whereby each O atom is linked to four O atoms of neighbouring molecules via four H-bonds, as illustrated in figure 1.5. This characteristic network, which implies a low coordination number of 4, essentially survives upon melting, at least locally, and explains many of the unusual properties of liquid water[4]. The example of the H-bond network in crystalline or liquid water shows that as simple a molecule as H_2O can already give rise to complex behaviour. More generally complex behaviour of liquid matter may often be traced back to one or several of the following characteristics of a given substance or material.

- Multicomponent systems, including mixtures of several molecular species and solutions, may give rise to compositional ordering or disordering and hence to fluid–fluid phase separation or demixing. The corresponding phase diagrams, which now involve the additional thermodynamic concentration variables characterizing the chemical composition, can rapidly become very complicated. In particular there may be a competition between condensation and demixing. However the step from pure, one-component simple fluids to mixtures of simple molecular species does not involve any new fundamental concepts. This is no longer true of mixtures involving charged (ionic) species, which are generally referred to as solutions.
- Ionic fluids involve at least two chemical species carrying electric charges of opposite sign, to ensure overall charge neutrality. The corresponding attractive and repulsive

---

[4] For example, the fact that the viscosity of liquid water *decreases* upon application of pressure, which disrupts the H-bond network and makes the system more fluid.

Coulomb interactions are of infinite ($1/r$) range, and give rise to highly collective behaviour like the Debye screening of the bare Coulomb forces, which will be discussed in section 3.10. The simplest ionic fluids are molten monovalent salts, which involve only oppositely charged anions (e.g. Cl^-) and cations (e.g. Na^+). The high melting temperature of most salts (e.g. $T_m = 1073$ K for NaCl) reflects the strength of the bare Coulomb attraction $e^2/4\pi\epsilon_0 r$ of an anion–cation pair. When a salt, or more generally an electrolyte, is dissolved in water, the anions and cations dissociate because their Coulomb interaction is reduced by a factor ϵ, where ϵ is the dielectric constant of water ($\epsilon \simeq 78$ at room temperature). The gain in entropy due to dissociation more than compensates for the reduction in the electrostatic attraction. Ionic solutions play a vital role in many chemical and biological processes. The strong coupling between ionic charges and the water dipoles leads to the hydration of individual ions by long-lived shells of water molecules. The strong electric field of the ions, or of strongly polar molecules, leads to polarization effects responsible for many-body induction forces. Microscopic ions also form electric double-layers near the highly charged surfaces of colloidal particles or other mesoscopic objects, which will be examined in section 7.6. Metals are another class of ionic systems, where the role of the anion is played by degenerate valence (or conduction) electrons. In many situations the metallic cations (e.g. Na^+, Ca^{2+} or Al^{3+}) and the neutralizing fraction of polarized valence electrons surrounding each cation, may be treated as 'pseudoatoms' interacting via short-range (screened), density-dependent pair potentials. The problem of liquid metal structure and thermodynamics is then similar to that of simple atomic liquids, apart from some additional twists due to the valence electron component, in particular as regards electronic transport properties (electric and thermal conductivities).

- Mesogenic substances. As long as it is not too far from spherical, molecular shape generally has no qualitative influence on phase behaviour of substances. However, sufficiently elongated (rod-like) or flat (plate-like) molecules may lead to additional anisotropic fluid phases, called liquid crystal phases. Such molecules are called mesogenic, and the new anisotropic phases, which are in some sense 'intermediate' between the isotropic liquid and the fully periodic crystal, are referred to as mesophases. The anisotropy gives rise to optical birefringence, as well as to peculiar elastic behaviour of liquid crystal materials. Some of the more common mesophases are shown schematically in figure 1.6. For rod-like molecules, these include the nematic, smectic A, smectic C and cholesteric phases, while plate-like molecules can form nematic and columnar phases. In the nematic phase, molecules are preferentially aligned along one direction, embodied in a unit vector **n**, called the director, thus breaking the rotational invariance of the isotropic phase, while translational invariance of the centres of mass is preserved. The director is an *order parameter* which plays a key role in the study of phase transitions (cf. chapter 4). Smectic (or lamellar) phases are characterized by orientational order, and the rods are organized in layers, with a one-dimensional periodicity in the direction perpendicular to the layers, thus breaking translational invariance in that direction; translational invariance is preserved inside each layer, along the two remaining directions. The distinction between smectic A and C phases is that in the former the director is along the normal to the layers, while it is tilted in the latter. In the cholesteric phase, the director rotates along an axis, thus leading to a helicoidal

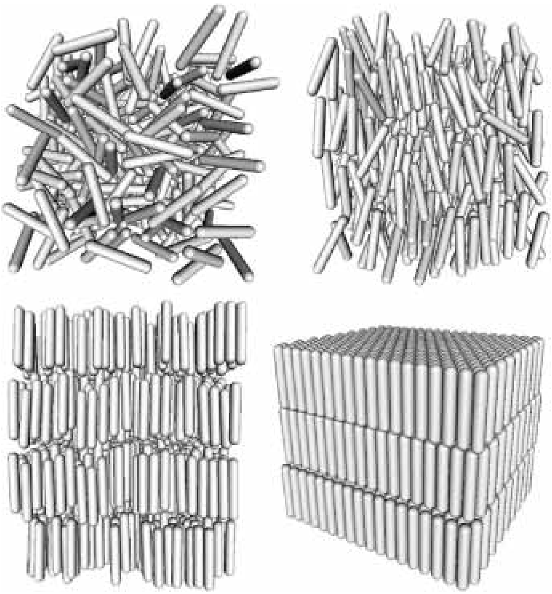

Figure 1.6. Typical configurations of the isotropic (upper left), nematic (upper right), smectic (lower right) and crystalline phases of a system of mesogenic molecules modelled as hard spherocylinders (i.e. cylinders capped by hemispheres of the same diameter). (Courtesy of P. Bolhuis.)

arrangement of rod-like molecules, with a pitch of typically a few hundred nm. Finally, in the columnar phase, flat (discotic) molecules are organized in parallel stacks or columns, the traces of which are ordered on a periodic two-dimensional hexagonal lattice, while the positions of the centres of the discotic molecules are disordered along the axes of the columns. The spontaneous shape-induced partial ordering of mesogenic molecules (see section 4.5) thus leads to much richer phase behaviour than shown in the standard phase diagrams in figure 1.1.

- Macromolecular systems. Whilst the mesogenic molecules considered above are fairly rigid, macromolecules of very high molecular weight (10^5 g/mol or more) are highly flexible objects. Linear polymers are chemically bonded chains of thousands of monomers, which can take on enormous numbers of different intramolecular conformations not unlike the many possible trajectories of an N-step random walk. A single long polymer chain is thus in itself a statistical object, a ‘coil’ which exhibits self-similarity, or scale invariance. This new type of symmetry means that macromolecular conformations are invariant under dilation, or change of scale, as illustrated in figure 1.7; this in turn implies that many characteristic properties of polymer chains may be expressed as simple power laws of the number N of monomers, provided $N \gg 1$. Simple models of polymer chains will be discussed in section 1.5. The study of a single polymer chain is relevant for the description of very dilute polymer solutions. Collective behaviour sets in in semi-dilute solutions, when neighbouring polymer coils begin to overlap, and even more in concentrated solutions or in solvent-free polymer melts, which exhibit complex dynamics. Chemical or physical cross-linking between different polymer chains can lead to the formation of a space-filling network called a gel, with peculiar viscoelastic properties intermediate between the elastic behaviour of a solid and the viscous flow of a simple liquid. The wealth of conformational,

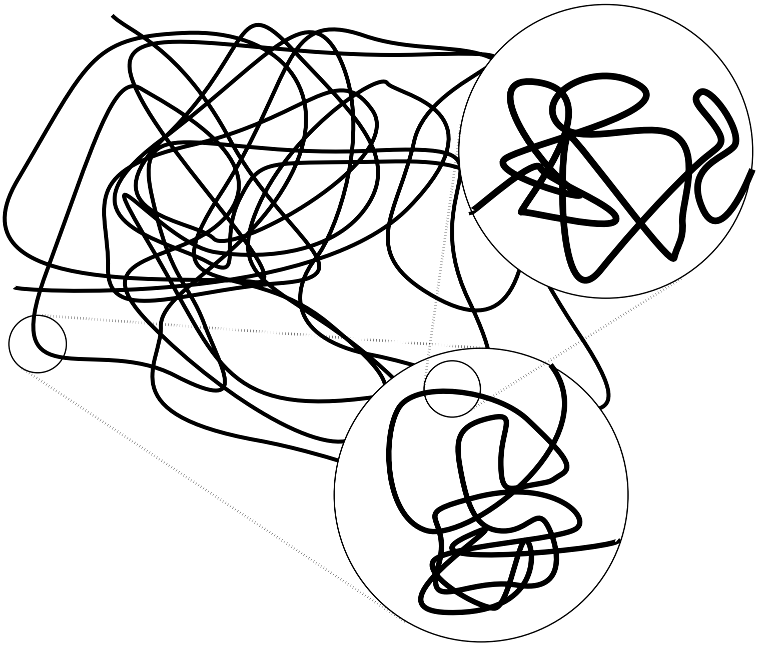

Figure 1.7. A typical conformation of a polymer coil, with two successive magnifications (cf. circular insets), illustrating scale invariance.

structural and dynamic behaviour is enhanced when one considers branched polymers, copolymers made up of several types of monomeric units, or polyelectrolytes, where monomers carry electric charges. Important examples are proteins, made up of random assemblies of 20 different amino-acid residues, or DNA, whose famous double-helix structure is an example of a particularly ‘stiff’ polyelectrolyte. These two macromolecules are key components of living cells, and significant ingredients of biological complexity.

- Self-assembly. Some large molecules have multiple chemical functionalities which strongly favour the spontaneous formation of supramolecular aggregates, a phenomenon often referred to as self-assembly. A first example are diblock copolymers, made up of two incompatible polymer chains, say A and B, linked together by a chemical bond. Since A and B chains do not mix, a solution or melt of diblock copolymers will lead to local phase separation into A-rich and B-rich microdomains, organized such as to minimize the contact between A and B segments. The second very important example is provided by amphiphilic molecules, or surfactants, like lipids made up of a polar head-group and one or several hydrocarbon chains. The head-group is hydrophilic, while the hydrocarbon tails are hydrophobic. When dissolved in water, such amphiphilic molecules will spontaneously form supramolecular aggregates called micelles, i.e. quasi-spherical assemblies with the hydrophilic heads at the surface, in contact with the solvent, while the hydrocarbon chains avoid being exposed to the water by clustering inside the micelle. The thermodynamics of micelle formation will be examined in section 2.6. Depending on their shape, lipids will minimize the contact between their hydrocarbon tails and water not by forming micelles, but rather by forming lipid bilayers, which are lamellar structures,

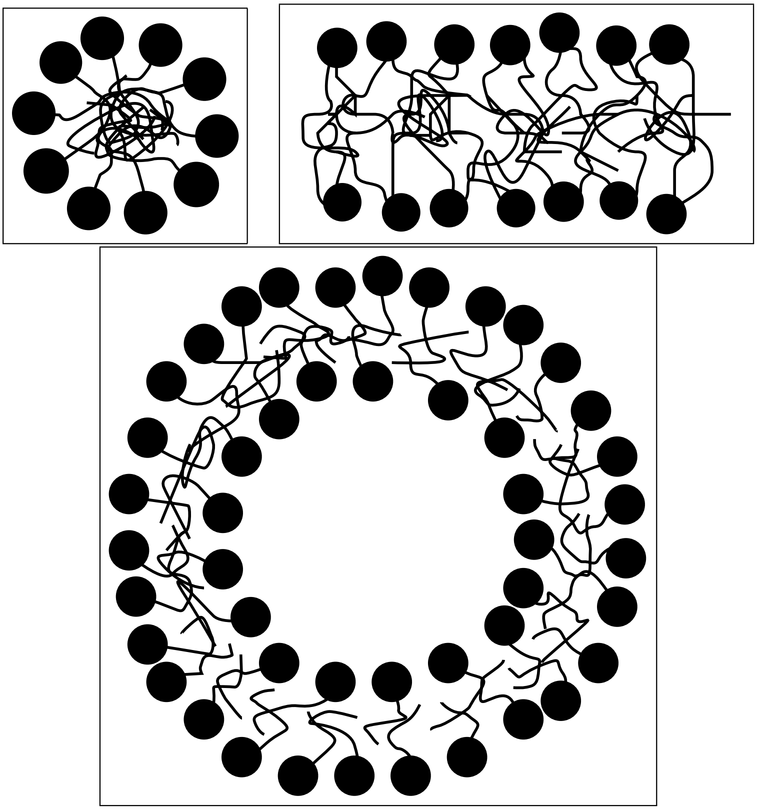

Figure 1.8. Schematic configurations of amphiphilic (surfactant) molecules, self-assembled into a micelle (upper left frame), a lamellar bilayer (upper right frame), and a vesicle (lower frame). The hydrophilic head-groups are represented by black circles, while the wiggly lines represent the hydrophobic tails; note that in the bilayer, each surfactant molecule has two tails.

as shown in figure 1.8. Contact of the hydrophobic alkane chains with water is again avoided by a spontaneous alignment of the tails inside the bilayer, while the polar heads point towards the solvent on both sides. The resulting flexible thin films are the simplest examples of biological membranes, the curvature elasticity of which is controlled by bending moduli (section 8.2). Depending on lipid concentration, and the energy cost of curvature, edge effects of planar bilayers may be avoided by the spontaneous formation of closed surfaces called vesicles, which are prototypes of living cells. The morphology of vesicles is essentially determined by their surface to volume ratio. Surfactant molecules will also spontaneously aggregate at the interface between immiscible water and oil, where they will tend to form monolayers, with the polar heads pointing to the water side and the hydrophobic alkane chain tails intruding into the oil phase. The surfactant molecules in fact reduce the strong surface tension of the liquid–oil interface, thus favouring the stability of microemulsions, which are mesoscopic two-phase systems of finely divided droplets of oil in water, or of water in oil, depending on the concentrations of the two liquids. Upon varying the concentration of surfactant, a large variety of microphases may be generated, including smectic lamellar phases, with alternating layers of oil and water, as well as more complex structures like bicontinuous phases where oil and water form interpenetrating domains separated by fully connected monolayer membranes spanning the whole volume of the sample.

- Suspensions and dispersions are highly heterogeneous two-phase (or multi-phase) systems, of which the previously mentioned microemulsions are a good example involving two liquid phases. Fog is another example involving finely divided water droplets suspended in air. More generally, *colloids* are dispersions of mesoscopic solid or liquid particles, with sizes ranging typically from tens to thousands of nanometres, in a suspending liquid. Colloidal dispersions, like ink, paints, lubricants, cosmetics, or milk, are ubiquitous in everyday life and play a key role in many industrial processes. Due to the highly divided nature, or high degree of heterogeneity, of a colloidal dispersion, the total surface separating the two constituent phases is very large, so that colloidal dispersions are dominated by interfacial properties. For example, 1 litre of a fairly concentrated suspension of spherical colloidal particles with a diameter of 10^2 nm, and a packing fraction $\phi = 0.1$, contains 2×10^{17} particles, and the total internal surface is about 1500 m^2! A widely studied category of colloidal dispersions involves mesoscopic solid particles, which may be crystallites, like naturally occurring silicates, or polymeric amorphous particles, like synthetic polystyrene or latex spheres, or small biological organisms, like viruses. Such solid colloids come in different shapes: spherical like the synthetic latexes, lamellar like clay platelets, or long rods, of which the tobacco mosaic virus (TMV) is a good example. It is then tempting to seek analogies between large assemblies of microscopic molecules forming various phases discussed earlier in this chapter, and suspensions of mesoscopic colloidal particles in a liquid. And indeed, colloidal dispersions are observed to give rise to various phases, including colloidal crystals and, in the case of rod-like particles, nematic phases, embedded in the suspending fluid. Quite apart from the difference in scale there are, however, a number of rather fundamental differences between molecular and colloidal assemblies. First of all, contrarily to molecules of a given species, which are all identical, colloidal particles have a size distribution, i.e. they are *polydisperse*; careful synthesis can limit relative differences in size to a few per cent in favourable cases, but size polydispersity is an intrinsic property of colloidal dispersions. A second, fundamental difference is the nature of particle dynamics: while the motions of interacting molecules are governed by reversible Newtonian dynamics, colloidal particles undergo irreversible Brownian dynamics due to their coupling to the suspending fluid; due to the very different time scales between the rapid thermal motions of the molecules, and the considerably slower motion of the much heavier colloidal (or Brownian) particles, this coupling can only be described in stochastic terms, as in the framework of the Langevin equation examined in section 10.1. A final, very significant feature of colloidal systems is that within a coarse-grained statistical description, where microscopic degrees of freedom are integrated out, the interaction between colloidal particles is an effective one, including an entropic component. In other words, the effective interaction energy between colloidal particles in a bath of microscopic molecules and ions, or in the presence of macromolecules, is a free energy, rather than a mere potential energy, and hence generally depends on the thermodynamic state variables (temperature, concentrations, etc. . .) of the suspension. Examples of such effective interactions include depletion forces, to be discussed in section 2.7, and the interactions between electric double-layers, associated with charged colloidal particles (cf. section 7.6). Finally, flow properties of concentrated dispersions generally deviate very significantly from the simple Newtonian behaviour of simple fluids, as embodied e.g. in equation (1.7) for a simple shear flow. The study of such non-Newtonian flow is the realm of rheology, and its many technological implications.

1.3 Exploring the liquid state

The present book describes some of the key concepts and models which have been developed to understand and predict the macroscopic and microscopic properties of liquids and their interfaces, in particular their structure and dynamical behaviour on molecular or mesoscopic scales. Ultimately the validity of theoretical predictions must be gauged against experimental measurements of such properties. Although later chapters will not dwell on experimental techniques, it is important to mention, at least briefly, some of the more widely used techniques, and the physical quantities to which they give access. Broadly speaking, the properties that are most frequently measured, and the corresponding experimental probes, fall into four categories, two of which are of macroscopic nature, while the other two relate more directly to the molecular or macromolecular constituents, on microscopic or mesoscopic scales.

- Thermodynamics characterizes macroscopic samples in equilibrium. The key bulk thermodynamic properties are the equation of state, compressibility and specific heat (at constant volume or pressure); they involve the measurement of the fluid density as a function of applied pressure, as well as various calorimetric techniques which also give access to latent heats at phase transitions. Free energies follow from thermodynamic integration, using basic thermodynamic relations which will be summarized in chapter 2. Solutions are characterized by their osmotic properties. In particular, the osmotic pressure Π exerted by the solute is traditionally measured by monitoring the rise of the solution in a vertical tube in osmotic equilibrium with the pure solvent across a semi-permeable membrane which allows the exchange of solvent molecules, but not of the solute. If h is the height to which the solution rises in the capillary, ρ_s the mass density of the solution, and g the acceleration of gravity, the osmotic pressure is $\Pi = \rho_s g h$. Osmometry is a direct application of osmotic equilibrium which allows the determination of the molar mass of macromolecules by measuring the osmotic pressure of a macromolecular solution.

  The static dielectric constant (or permittivity) ϵ is another important macroscopic property of a fluid, which determines the response of a sample, in the form of the electric polarization $\mathbf{P}$, to an externally applied electric field, or corresponding displacement field $\mathbf{D}$. The field $\mathbf{E}$ inside the sample is related to $\mathbf{D}$ via the relation

$$\mathbf{D} = \epsilon_0 \mathbf{E} + \mathbf{P} = \epsilon\epsilon_0 \mathbf{E} \tag{1.12}$$

  where the second equality is valid in the linear regime. ϵ is a scalar if the fluid sample is isotropic, and ϵ_0 is the permittivity of empty space. ϵ is thus directly determined by measuring the electric field inside a condenser in the absence and in the presence of the fluid sample. The dielectric constant is state dependent, and a high value will ensure strong dissociation of electrolytes in highly polar solvents, like water. Another important application of equation (1.12) is the propagation of light, since ϵ (which depends on the frequency) is related to the index of refraction. In anisotropic, complex fluids, birefingence (i.e. the dependence of the index of refraction on the polarization of light) yields important information on molecular orientations.

Interfacial phenomena are dominated by the surface tension, a force per unit length (or energy per unit area), which may be measured by a number of techniques, based on the Young–Laplace equation for the pressure drop across a curved interface (cf. section 6.4)

$$\Delta P = \gamma \left(\frac{1}{R_1} + \frac{1}{R_2} \right) \tag{1.13}$$

where R_1 and R_2 are the curvature radii of the dividing surface (see section 6.2). A classic technique is based on the measurement of the angle made by the meniscus of the liquid–gas interface in a capillary rise experiment. Related methods are based on digital image analysis of the shape of drops or bubbles under gravity (sessile drop or bubble method). The thickness of interfaces or adsorbed thin liquid films is routinely measured by ellipsometric methods analysing the elliptical polarization of light beams reflected by interfaces or films. Similar information may be derived from X-ray reflectivity measurements.

- Macroscopic transport coefficients determine the dissipative (irreversible) behaviour and the flow properties of fluids. The thermal and electrical conductivities determine the heat and charge currents through a fluid subjected to gradients in temperature or electric potential, while the shear and bulk viscosities, η and ζ, characterize the internal friction in a flowing Newtonian fluid, obeying a linear relationship between stress and strain rate (cf. equation (1.7)). Standard viscosimeters measure η, either by monitoring fluid flow through capillaries or by using rotating coaxial cylinders; in the latter experiment, the viscosity of a fluid placed between an outer and an inner cylinder is directly determined by measuring the torque exerted on the inner cylinder, when the outer cylinder is rotated at constant angular velocity. A combination of η and ζ determines the attenuation of sound waves propagating though a liquid (cf. section 11.5). The vast field of rheology explores the flow properties of complex fluids, including polymer solutions and melts, and colloidal dispersions or various other suspensions. Such fluids are generally non-Newtonian, i.e. the stress versus strain rate relation is no longer linear. In particular, Bingham fluids flow only beyond a threshold of applied stress (the yield stress). Suspensions often exhibit thixotropy, i.e. the reduction of viscosity at higher flow rates ('shear thinning'). A well known illustration is the reduction of the viscosity of paints by brushing. Despite its obvious technological importance, the rheological behaviour of complex fluids will not be considered further in this book.
- Shifting the attention to mesoscopic and molecular scales, a key objective is to characterize the static local structure of fluids, i.e. the average spatial organization of the basic constituents (molecules, macromolecules or supramolecular aggregates). The spatial arrangement may be described by a set of static correlation functions, of which the pair distribution function $g(r)$, already introduced in section 1.1 (cf. equation (1.2))

is the simplest and most studied. In fact, as will be shown in more detail in section 3.8, the spatial Fourier transform of $g(r)$, called the static structure factor $S(k)$ (where the wavenumber k is the variable conjugate to r), is directly accessible to radiation diffraction experiments. If molecular scales (of the order of a nanometre or less) are to be probed, the natural radiations are X-rays or thermal neutrons from reactors or spallation sources, because their wavelength is of the order of angstroms. The availability of very intense X-ray sources from synchrotron radiation makes it possible to obtain time-resolved diffraction patterns, allowing e.g. the evolution of non-equilibrium and metastable structures (like those of glassy materials) to be monitored on time scales of a fraction of a second. If mesoscopic structures are to be explored, as in colloidal suspensions, X-rays and neutrons may still be used, provided that the diffractometers can resolve very small wavenumbers; as will become clear in section 3.8, this corresponds to the regime of small angle scattering. Alternatively one may use radiations of longer wavelengths, like visible light which is diffracted by assemblies of particles of colloidal size, or one can resort to direct visualization using a powerful microscope; this is combined with video recordings in the widely used technique of video microscopy. Diffraction measurements are generally applied to local order determinations of bulk fluids, on the assumption of homogeneity or translational invariance. Inhomogeneous fluids and interfacial regions break translational invariance, and are hence characterized by a spatially varying local density (or density profile), rather than by a mere constant bulk number density ρ. Such density profiles $\rho(\mathbf{r})$ are accessible in X-ray or neutron reflectivity experiments, and by grazing incidence X-ray diffraction. The interfacial structure, and in particular the layering of molecules in strongly confined fluids, e.g. near a solid wall, may also be measured by a surface force apparatus, capable of measuring forces between plates induced by very thin fluid films, on the nanonewton scale, with a spatial resolution of the order of an angstrom. The same apparatus is also well adapted to investigate lubrication forces and capillary condensation, as well as various aspects of wetting phenomena (sections 6.3, 6.4).

- Experimental investigations of individual or collective motions of molecules or particles require the use of dynamical, time or frequency-dependent probes. One of the most widely used dynamical diagnostics is inelastic scattering of neutrons or photons. Since thermal neutrons have energies comparable to the kinetic energy of molecules in fluids, the inelastic scattering cross-section contains detailed information on molecular motions (cf. section 11.6). Inelastic or quasi-elastic scattering of light probes length scales of the order of the wavelength of light, and is hence well adapted to examine collective dynamical fluctuations in molecular fluids (as in Rayleigh–Brillouin scattering), or the motion of mesoscopic colloidal particles. Dynamics of the latter may also be explored by photon correlation spectroscopy, an interferometric method well adapted to slow relaxation processes, typically in the range of milliseconds. Slow diffusion of molecules and macromolecules, on the scale of microseconds, can be resolved by nuclear magnetic resonance (NMR, section 11.7), while reorientational motions of molecular dipoles are conveniently measured by dielectric relaxation (section 10.3). Detailed information of how intermolecular forces affect the rotational and vibrational motions of molecules in liquids, as compared to their gas-phase behaviour, may be gained from various spectroscopic techniques, including infrared (IR) and Raman spectroscopy, which are beyond the scope of this presentation.

To conclude this introductory chapter it seems worthwhile to illustrate two of the key concepts in complex fluids, namely free volume and scale invariance, by simple examples, before embarking on a more systematic presentation in the following chapters. As a third example, we shall briefly show how computer simulations of atomistic models can provide extremely valuable information on the structure, phase behaviour and dynamics of simple and complex fluids, supplementing the data obtained from experimental probes.

1.4 Application 1: excluded and free volume

The single most important feature of the interaction between molecules or colloidal particles is their strong mutual repulsion whenever their centres come within a distance of the order of the particle diameter. For non-spherical particles, this shape-dependent repulsion will obviously be a function of the mutual orientation of the molecules, and this will be a very important factor e.g. in the case of liquid crystals. For the sake of clarity, we shall first restrict the discussion to spherical particles of diameter $\sigma = 2R$. In view of the steepness of the repulsive potential between two such particles, the latter may very often, to a good approximation, be regarded as non-interpenetrating hard spheres, such that the interaction 'potential' is simply $v(r) = \infty$, $r < \sigma$ and $v(r) = 0$, $r > \sigma$. The corresponding Boltzmann factor reduces to a Heaviside step function

$$\exp(-\beta v(r)) = \theta(r - \sigma) \tag{1.14}$$

where $\theta(x) = 1(0)$ if $x > 0(< 0)$. Note that the Boltzmann factor for a pair of hard spheres is independent of temperature; this is a direct consequence of the absence of any energy scale in a hard sphere fluid, and is a common characteristic of athermal systems made up of particles having only excluded volume interactions. In the case of hard spheres, the excluded volume around the centre of any particle is that of a sphere centred on that particle and of radius equal to the particle diameter σ, so that the excluded volume $v_{\mathrm{ex}} = 4\pi\sigma^3/3$ is eight times the volume $v_0 = 4\pi R^3/3$ of the particle itself. Each particle has such an exclusion sphere associated with it, as shown in the equivalent two-dimensional situation in figure 1.9. The centre of any additional (or test) particle inserted into the fluid cannot come closer than σ to the centres of the existing spheres, and hence cannot penetrate into the exclusion spheres around the latter. It is important to realize that, while the excluded volume associated with each individual sphere is v_{ex}, the total volume V_{ex} from which the centre of a test sphere is excluded is less than $N \times v_{\mathrm{ex}}$, since the exclusion spheres of neighbouring particles can overlap, as illustrated in figure 1.9. The volume accessible to a test particle is simply the total volume of the system minus the excluded volume, $V' = V - V_{\mathrm{ex}}$. V_{ex}, and hence V', depend on the instantaneous configuration of the N non-overlapping particles; V_{ex} fluctuates as the positions $\mathbf{r}_i$ $(1 < i < N)$ of the spheres vary in

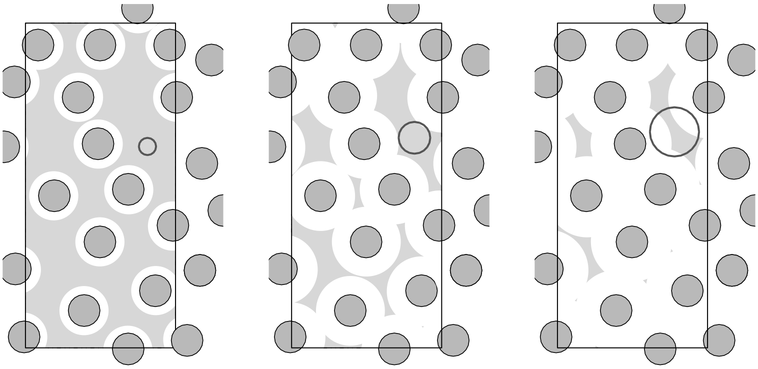

Figure 1.9. Schematic two-dimensional representation of free (or accessible) 'volume' (area in this case) for typical fluid-like configurations of hard discs. The test particle is shown as a heavy-lined circle; the hard discs are the dark grey circles; the concentric white areas represent the excluded area around each disc. As the diameter of the test particle increases (from left to right), so does the diameter of each exclusion circle; the light grey area represents the free area, accessible to the centre of the test particle without causing overlap with any of the discs; the free area is shown only within the rectangular frames. (Courtesy of D. Goulding.)

time, due to their thermal motion. The value of the accessible volume V' averaged over all allowed configurations of spheres is called the free volume. Allowed configurations are such that $|\mathbf{r}_i - \mathbf{r}_j| > \sigma$ for all $N(N-1)/2$ pairs of particles. Bearing in mind that the test particle is identical to the spheres in the system, it will be shown later (section 2.5) that V_{ex} is intimately related to the chemical potential of a hard sphere fluid. Meanwhile we consider two limiting cases. At very low densities, the volume per particle $v \gg v_{\text{ex}}$, so that the overlap of the exclusion volumes associated with different particles is very unlikely. In that case the volume accessible to the test particle, which may be identified with any one of the spheres, is simply $V' = V - Nv_{\text{ex}}$. The phase space volume for one sphere is $\omega = (V - Nv_{\text{ex}})/\Lambda^3$, where

$$\Lambda = h/\sqrt{2\pi m k_{\text{B}} T} \tag{1.15}$$

is the de Broglie thermal wavelength, stemming from the integration over a Maxwell distribution of momenta for particles of mass m, and h is Planck's constant. The total phase space volume, or partition function, for hard spheres is then approximately given by

$$\Omega = \frac{(V - Nv_{\text{ex}}/2)^N}{N!\Lambda^{3N}} \tag{1.16}$$

The factor $1/2$ occurs to avoid double-counting of the excluded volume for pairs of spheres. The entropy finally follows from Boltzmann's relation

$$S = k_{\text{B}} \ln \Omega = Nk_{\text{B}} \ln\left(\frac{v - v_{\text{ex}}/2}{\Lambda^3}\right) \tag{1.17}$$

where Stirling's formula $\ln N! \simeq N \ln N - N$ has been used. In an athermal system, the Helmholtz free energy reduces to $-TS$, and the pressure follows from

$$P = -\left(\frac{\partial F}{\partial V}\right)_{N,T} = T\left(\frac{\partial S}{\partial V}\right)_{N,T} = \frac{k_{\mathrm{B}}T}{v - v_{\mathrm{ex}}/2} \tag{1.18}$$

The dimensionless compressibility factor (or equation of state) reduces to

$$Z = \frac{PV}{Nk_{\mathrm{B}}T} = \frac{1}{1 - 4\phi} \tag{1.19}$$

where $\phi = \pi\sigma^3/6v$ is the packing fraction for hard spheres. Note that (1.19) can only be expected to be valid for $\phi \ll 1$, so that to lowest order in ϕ, $Z = 1 + 4\phi + \mathcal{O}(\phi^2)$; the term linear in ϕ is the leading correction to the ideal gas law in a *virial* expansion of Z in powers of the density $\rho = 1/v$. In the opposite limit of high densities, which is much more relevant for the condensed (liquid or solid) states of matter, calculation of the free volume is a much more difficult task, due to the numerous overlaps of the excluded volumes associated with each particle. On average each particle is trapped in a cage of neighbouring spheres, and the free volume per particle $v' = V'/N$ is much less than the volume per particle $v = V/N$.

The free volume v' accessible to any one particle trapped in its cage may then be calculated with a *cell model*, whereby the nearest neighbours of the particle are assumed to be fixed at some favourable average position. In a crystal, the average positions naturally coincide with the lattice positions of the first coordination shell of nearest neighbours around the trapped particle. The very concept of an average position of molecules is meaningless in fluids, since the molecules diffuse away from any initial position, according to Einstein's law (1.8). However, on a sufficiently short time scale, say 1 ps, a small molecule will have moved typically less than 0.1 nm in a dense fluid, so that the neighbours forming the cage may be considered as effectively 'frozen' for the purpose of calculating the free volume v'. For the sake of an easier graphical free volume representation, we consider in figure 1.10 the two-dimensional case of hard discs. The most compact packing is achieved by the triangular lattice, where each atom is surrounded by six nearest neighbours placed at the vertices of a hexagonal cell, at a distance $d = (2/\sqrt{3}\rho)^{1/2}$ from the centre, where ρ is the number of atoms per unit area (number density of the system). The free area available to the atom within the hexagonal cage is the shaded area in figure 1.10, resulting from the intersection of the exclusion discs of radius $\sigma = 2R$ centred on each of the six vertices. For dense fluids, d is only slightly larger than σ, and an elementary calculation leads to a simple expression for the free area, valid to second order in $(d/\sigma - 1)$, namely $a' = 2\sqrt{3}(d - \sigma)^2$. The resulting entropy is $S = Nk_{\mathrm{B}} \ln[2\sqrt{3}(d - \sigma)^2/\Lambda^2]$ and